

OPEN ACCESS

Repository of the Max Delbrück Center for Molecular Medicine (MDC)
Berlin (Germany)
<http://edoc.mdc-berlin.de/14252/>

Crystal structure of the yeast TRAPP-associated protein Tca17

Wang, C., Gohlke, U., Roske, Y., Heinemann, U.

This is the accepted version of the following article:

Wang, C., Gohlke, U., Roske, Y., Heinemann, U. Crystal structure of the yeast TRAPP-associated protein Tca17. FEBS Journal 281(18): 4195-4206, 2014.

which has been published in final form at <http://dx.doi.org/10.1111/febs.12888>

John Wiley & Sons, Inc. ►

Crystal structure of the yeast TRAPP-associated protein Tca17

Chengcheng Wang^{1,2}, Ulrich Gohlke¹, Yvette Roske¹, and Udo Heinemann¹

¹Macromolecular Structure and Interaction Group, Max-Delbrück-Center for Molecular Medicine, Robert-Rössle-Str. 10, 13125 Berlin, Germany, and Chemistry and Biochemistry Institute, Freie Universität, Takustr. 6, 14195 Berlin, Germany

²Present address: Crown Bioscience Inc., Science & Technology Innovation Park, No.6 Beijing West Road, Taicang City, Jiangsu Province, P.R. China 215400

Corresponding author: Udo Heinemann, Max-Delbrück-Center for Molecular Medicine, Robert-Rössle-Str. 10, 13125 Berlin, Germany, Tel.: 0049 30 9406 3420, Fax: 0049 30 9406 2548, Email: heinemann@mdc-berlin.de

Keywords: TRAPP, vesicle transport, Tca17, Trs20, Sedlin

Abstract

The transport protein particle (TRAPP) is a hetero-multimeric complex involved in the trafficking of COP II (coat protein complex-II) vesicles. TRAPP is present in different eukaryotes from yeast to vertebrates and occurs in three distinct modifications with function in different intracellular transport steps. All forms contain a core of five essential subunits, and the different species of TRAPP are formed by the addition of various subunits. A recently identified TRAPP-associated protein, Tca17, is supposed to be involved in the regulation of the transport complex. We have determined the three-dimensional structure of yeast Tca17 by X-ray crystallography at a resolution of 1.8 Å. It adopts the longin fold characteristic for the Bet5 family of TRAPP subunits, and it also shares a binding motif of these for the interaction with other members of the complex. Two alternative models of the localization of Tca17 within TRAPP as well as its potential role in the regulation of TRAPP function by transient integration into the complex are discussed.

Database: Structural data are available in the Protein Databank (PDB) under the accession number 3PR6.

Introduction

Cargo transport across and between the membranes of eukaryotic cells relies on vesicles, small containers enclosed in membrane bilayers that facilitate transport following anterograde (secretory) and retrograde pathways. The molecular machinery that carries out central functions in vesicular transport is functionally conserved across all eukaryotic species and between individual transport steps [1]. Vesicular transport between a cellular donor and an acceptor compartment follows a series of distinct steps starting with cargo recruitment at the donor membrane, followed by vesicle budding, release and uncoating, and ending with vesicle tethering at the acceptor membrane, SNARE protein pairing, membrane fusion and cargo release [2]. Each transport event encompassing these steps is thought to be carried out by a functional module of the cell [3].

Upon vesicle tethering, first physical contact is established between the transport container and the target membrane. Tethering depends on three classes of proteinaceous factors: A small GTPase of the Rab/Ypt family that travels with the vesicle, one or more proteins with extended coiled-coil regions anchored at the target membrane, or a multi-subunit tethering complex recruited to the target membrane and composed of soluble components [4-6]. Secretory COP II vesicles formed at the endoplasmic reticulum are tethered to the *cis*-Golgi membrane by the GTPase Rab1 (Ypt1 in yeast), the golgin p115 (Uso1 in yeast) and the transport protein particle (TRAPP).

TRAPP is a large multisubunit complex of which three forms have been identified in yeast, each having a unique composition and showing a particular function in the vesicular transport pathway [7]. In mammals, the number and composition of TRAPP complexes is less clear, but orthologous subunits have been identified, and there is evidence for distinct TRAPP complexes to be involved in the regulation of mammalian ER-to-Golgi traffic [8]. TRAPP I contains at least five subunits (mammalian nomenclature in parentheses), Bet3-A, Bet3-B (TRAPPC3, 3L), Bet5 (TRAPPC1), Trs23 (TRAPPC4), and Trs31 (TRAPPC5). TRAPP I acts as a GTP exchange factor (GEF), and it recognizes and binds ER-derived COP II vesicles to the Golgi apparatus [9-11]. Two subunits, Trs20 (TRAPPC2, Sedlin) and Trs33 (TRAPPC6, 6a, 6b) are required for the assembly of the TRAPP-II complex which, in addition to the TRAPP-I core, contains three proteins, the non-essential Trs65 (TRAPPC13), Trs120 (TRAPPC9), and Trs130 (TRAPPC10) [12]. The latter two shift the tethering specificity of the mammalian TRAPP complex from COP-II to COP-I coated vesicles, presumably through direct interaction with γ 1COP, a COP-I coat adaptor protein [13]. Structural studies by X-ray crystallography of various TRAPP sub-complexes from mammals [14] and yeast [15] have led to the following composite picture of yeast TRAPP I architecture:

The complex forms an elongated structure of ca. 180 Å length, resting flat on the cytosolic side of the Golgi membrane. Two hetero-trimeric sub-complexes consist of Bet3-A, Trs33 and Bet5 on the one side, and of Bet3-B, Trs31 and Trs23 on the other side. The interface between the two halves of the TRAPP I complex is formed by Bet5 and Trs23, which are related by a pseudo two-fold symmetry axis oriented perpendicular to the membrane. An additional subunit, Trs20 (Sedlin in mammals), binds to Trs31. The complex is thought to associate with the membrane via Bet3-A/B, since no other anchoring protein could be identified so far [16, 17]. Very little is known about the quaternary structure of TRAPP II. A recent EM study of the complex from yeast containing all subunits shows a diamond-shaped structure formed by the dimerization of two nine-component core complexes [18]. However, the exact arrangement of the components of TRAPP II is unresolved with at least four models under discussion [19].

A third complex, TRAPP III, has been identified as acting in autophagy, and it contains the TRAPP I components and additionally the TRAPP-III specific subunit Trs85 (TRAPPC8) [20, 21]. Structure analysis by EM has shown that TRAPP III is formed by the attachment of Trs85 to the Trs20-binding end of the elongated TRAPP-I structure [22].

Recently, an additional member, Tca17, of the yeast TRAPP complex was identified. Tca17 is proposed to be a component of TRAPP II and to promote the assembly and stability of the complex through interaction with Trs33 and Trs130 [21, 23]. A similar result was reported for its human

ortholog, TRAPPC2L [24]. Based on sequence similarity, TRAPPC2L is remotely related to the TRAPP subunit Sedlin which is grouped in the same family of small TRAPP subunits as Bet5 and Trs23 [6].

Here we have determined by X-ray crystallography the three-dimensional structure of Tca17 from yeast at a resolution of 1.80 Å. It shows that Tca17 indeed adopts the longin fold characteristic for the Bet5 subfamily of TRAPP subunits. It is most closely related to Trs20/Sedlin, and its surface properties suggest that it can bind to other TRAPP subunits. Its role in the regulation of TRAPP function by transient integration into the complex is discussed.

Results and Discussion

Crystal structure analysis of Tca17 from yeast

The coding region for full-length Tca17 (residues 1-152) from yeast was heterologously expressed in *E. coli* and purified utilizing an N-terminal GST-affinity tag, followed by removal of the tag and size exclusion chromatography. The crystal structure of Tca17 was determined by multi-wavelength anomalous diffraction (MAD) at a resolution of 1.80 Å. Tca17 crystallizes in space group C2 with one molecule per asymmetric unit. 141 out of 152 amino acid residues of Tca17 could be traced in the electron density, while two residues at the N-terminus as well as the loop connecting strand β 2 and helix α 1 (Fig. 1) could not be modeled, probably due to local disorder. At the C-terminus of the protein, two additional amino acids derived from the cloning vector could be fitted into the electron density.

As a member of the Bet5 subfamily of TRAPP complex subunits, Tca17 shows a longin-like fold, where a central β -sheet formed by five anti-parallel β -strands is flanked by one α -helix (α 1) on one side (“one-helix side”, Fig. 1A) and two α -helices (α 2, α 3) on the opposite side (“two-helix side”, Fig. 1B). In contrast to other Bet5-like proteins, the C-terminus of Tca17 extends beyond helix α 3 and forms an additional short helix α 4, which points away from the rest of the protein, but it is stabilized by crystal contacts with a symmetry-related molecule. Besides two hydrogen bonds, the interface involves mostly hydrophobic interactions between several leucine and valine side-chains. This interface includes, however, non-native residues derived from the cloning process of the protein and is therefore unlikely to be physiologically relevant. Another interface is formed with a second molecule related by the two-fold rotation axis. Here, the Cys121 side-chains of the two molecules are covalently linked by a disulfide bond. We assessed therefore the oligomerization state of Tca17 in solution by a number of orthogonal assays such as sedimentation velocity experiments through analytical ultracentrifugation, analytical size exclusion chromatography combined with static light scattering (SLS), and SDS-PAGE, all under reducing and non-reducing conditions. Even in the absence of a reducing agent, more than 95% of Tca17 was observed to exist in the monomeric form in all

experiments (data not shown). Finally, analysis of the interface between the two monomers [25] renders a Tca17 dimer in the absence of a disulfide bond under physiological conditions in the cytosol rather unlikely.

Comparison of Tca17 with members of the TRAPP complex

The protein pair of Tca17 (TRAPPC2L in mammals) and Trs20 (TRAPPC2/Sedlin in mammals) is found in a variety of eukaryotic species, suggesting a distinct and conserved function for either protein. Recent studies have shown that Trs20 is required for assembly of the TRAPP II complex and that it is essential for the viability of yeast cells [19]. It is also essential for TRAPP III formation, and mutation of Trs20 leads to defects in TRAPP III-dependent autophagy [26]. A similar role as an adaptor for TRAPP assembly was shown for the mammalian ortholog TRAPPC2 [27, 28]. To understand the function of Tca17 on the basis of sequence conservation, Tca17 orthologs from eighteen different species, including the well characterized orthologs from metazoans as well as several hypothetical proteins from yeasts, were aligned using Clustal Omega [29]. Sequence conservation was subsequently analyzed using ConSurf [30]. The normalized ConSurf score for each residue in the multiple sequence alignment (Fig. 2) is a relative measure of evolutionary conservation, with the lowest score representing the most conserved position in a given protein family. The structure of Tca17 colored according to sequence conservation is shown in Fig. 3A. In general, Tca17/TRAPPC2L is less conserved than Trs20/TRAPPC2 [24], as expected for a protein which is not involved directly in the function of the TRAPP complex, but rather serves in a regulatory role. The majority of the most conserved residues are found in the hydrophobic core of the lower part of Tca17 (Fig. 3A). Distribution of main-chain atomic displacement factors also suggests low internal flexibility in this part of the protein. Taken together, maintaining a stable fold in this region seems to be important for the function of Tca17. In addition, two distinct conserved patches can be identified on opposite surfaces of Tca17 (Fig. 3B).

As a member of the Bet5 subfamily of TRAPP subunits, Tca17 shares a longin-like fold with Sedlin, Bet5, and Trs23. This raises the possibility that Tca17 is integrated into the TRAPP complex in place of any of these three TRAPP subunits. Since a regulatory function of Tca17 is expected to result from protein-protein interactions, the electrostatic potential distributions of the four Bet5 subfamily members were computed for comparison, and they are shown in Fig. 4 with the proteins in the same orientations of their longin-like core structures. For Tca17 the picture is qualitatively similar to that of Sedlin, but clearly different from Bet5 and Trs23, particularly on the one-helix side. Here, Tca17 as well as Sedlin show a widely spread area of negative charge, with a concentrated patch that is for Sedlin located on the presumably cytosolic side of the TRAPP complex, and therefore open for protein-protein interactions, e.g. with SNARE proteins such as Syntaxin 5 [14, 28, 31]. This area is

highly conserved among Tca17/TRAPPC2L proteins from various species (patch 1 in Fig. 3B) as well as in comparison with the TRAPPC2 protein family, suggesting an important interaction site [23, 24]. Indeed, Trs20 facilitates the assembly of both TRAPP II and III through interaction with Trs120 and Trs85, respectively, and the mutation Asp46Tyr abolishes this [19, 26-28]. Mutation of the equivalent residue (Asp47) in human Sedlin is one of the causes leading to the X-linked skeletal disorder *spondyloepiphyseal dysplasia tarda* (SED) [32, 33], which underlines the importance of this region for the functionality of the TRAPPC2/C2L family. When the structures of Tca17 (Leu44-Asp45) and Sedlin (Leu46-Asp47) are superimposed, these residues are located at similar positions on the protein surface, and the orientation of their side-chains is similar (Fig. 5), suggesting that this spot serves as a specific protein binding site. Looking from the two-helix side, Tca17 and Sedlin appear less similar (Fig. 4). While the surface of Sedlin is mostly neutral, with only a few spots of positive charge, Tca17 shows a distinct negative patch, composed of the β 2- α 2 loop and the beginning of helix α 2.

Localization of Tca17 in the TRAPP II complex

Cell-biological studies have raised two possibilities for the integration of Tca17 into yeast TRAPP complexes (Fig. 6). First, Tca17 could be co-purified with a Bet3-Trs31 hetero-dimer [24], indicating a presumably transient replacement of Trs20 in TRAPP. After docking of the coordinates of Tca17 into the present model of TRAPP I [14] in the same orientation as it is found for Sedlin (Tca17-A, Fig. 6A), it is evident that, if Tca17 is indeed integrated into TRAPP in place of Sedlin/Trs20, a strong negatively charged area is created on the surface of TRAPP facing the membrane and presumably weakening the association with it (Fig. 6B). We notice, however, that this region of Tca17/TRAPPC2L is only weakly conserved (Fig. 2), implying a non-essential function. The negative patch also extends further to the side of the protein which is facing away from the TRAPP I core (Fig. 6C). This end of TRAPP would be capped by the TRAPP II-specific subunit Trs130 in the EM-derived yeast TRAPP II model [18]. The co-localization of Tca17 and Trs130 has been shown [23, 28], and it seems possible that this patch on the surface of Tca17 links it with the TRAPP II complex.

In a second scenario for its interaction with TRAPP, Tca17 binds in a position between Bet3 and Trs33 at the opposite end of the complex which is related by a pseudo two-fold symmetry to the binding site of Sedlin (Tca17-B, Fig. 6A) [21]. This is corroborated by co-precipitation experiments that have shown the interaction of Tca17 with Trs33 in yeast [23] as well as of the human orthologs TRAPPC2L and TRAPPC6a [24]. In the latter study, co-IP experiments also suggest that TRAPPC2 and TRAPPC2L both reside in the same TRAPP complex rather than replace each other. Docking of our Tca17 coordinates into the TRAPP I model in this position creates a similar negatively charged patch on the putative membrane-facing side of the complex as the replacement model with Trs20 does (Fig. 6B,C).

While in the EM-derived TRAPP II model [18], this end of the complex is capped by Trs120, an alternative model following two-hybrid analysis and co-purification/-immunoprecipitation experiments suggests the direct interaction of Tca17 with the N-terminal region of Trs130 at his position [21, 28]. Finally, Tca17 has not been detected yet in the TRAPP III complex, and in a *tca17Δ* yeast strain neither assembly nor function of the complex are affected [22, 26, 28]. Therefore, Tca17 does not seem to be an essential subunit of TRAPP III or, indeed, to interact with Trs85 in exchange of Trs20.

The crystal structure of Tca17 allows us to predict and analyze possible interactions with TRAPP I-core subunits such as Bet3, Trs31 or Trs33 on a molecular level. The predicted Bet3-interaction site of yeast Tca17 in comparison to the same site of mammalian Sedlin is shown in Fig. 7A. The interaction motif is relatively conserved (Sedlin: ¹¹¹MNPF, Fig. 7B, Tca17: ¹²¹CNPL, Fig. 7C), corresponding to patch 2 in Fig. 3B. Being located between helix α 2 and helix α 3, it is accessible to protein binding by protruding from the structure of Tca17. In the crystal structure of Tca17, Cys121 is involved in disulfide bond formation. However, as discussed above, this is likely to be a crystallization artifact, and under reducing conditions in the cytosol this residue is expected to be accessible for interactions.

While the binding modes between Tca17 and either Bet3-A or Bet3-B in the two alternative models described above are expected to be very similar, the interactions of Tca17 with Trs31 and Trs33 must be different. Fig. 8 shows the interfaces of the putative binding partners together with the surface patch of Sedlin that faces Trs31 in the TRAPP I model (see Fig. 6A). The charge distribution on the solvent-accessible surfaces of Trs31 and Trs33 are clearly different, with a unique negative area on the latter that might be matched by a corresponding positive patch on Tca17. However, this does not allow to decide for or against one of the proposed models. Also, no sequence conservation between Sedlin and Tca17 can be found here, while the interface of Sedlin and Trs31 is maintained through a number of hydrogen bonds (data not shown). In absence of a complex structure, it is not possible to find conclusive evidence on a molecular level for the interaction of Tca17 and Trs31 or Trs33.

Conclusion

We have determined the three-dimensional structure of the formerly little known yeast TRAPP-associated protein, Tca17. Though not previously identified as a TRAPP subunit, Tca17 as well as its mammalian ortholog TRAPPC2L were described to be sub-stoichiometric components of TRAPP II and to promote the assembly and stability of the complex. The crystal structure analysis at 1.8 Å resolution shows that Tca17 adopts the longin fold characteristic for the Bet5 subfamily of small TRAPP subunits. On the sequence and structure level, Tca17 is most closely related to the TRAPP subunit Trs20p/Sedlin. In addition, Tca17 shares a characteristic sequence motif with Trs20/Sedlin for the

interaction with Bet3. Transient integration of Tca17 into TRAPP, either replacing Trs20 or as an additional subunit would create a negatively charged patch on the suggested membrane association interface of the complex which might explain the role of Tca17 in the regulation of TRAPP-mediated vesicle tethering. On the other hand, residues found to be essential in Trs20/Sedlin for protein-protein interactions that lead to the assembly of TRAPP II and TRAPP III complexes are strictly conserved on the sequence as well as the structure level suggesting a related function for Tca17. In accordance with a number of recent cell-biological studies, our analysis of the structure of Tca17 points towards a role as an adaptor protein in TRAPP II assembly possibly by interacting with Trs130 and complementary to the interaction of Trs20 and Trs120. Further experiments, including the molecular and structural analysis of sub-complexes, are needed to validate the proposed interactions of Tca17 with members of the TRAPP complex.

Material and Methods

Expression cloning and protein purification of Tca17

The coding region for full-length Tca17 (residues 1-152) was amplified directly from yeast genomic DNA and cloned into the bacterial expression vector pGEX-6P1 using BamHI/NotI restriction endonucleases. After transformation of *E. coli* BL21 (DE3)-T1R cells with the recombinant plasmid pGEX6-P1-Tca17, large-scale gene expression was induced by addition of 0.1 mM isopropyl-1-thio- β -D-galactopyranoside (IPTG) to LB medium, and cells were harvested after growing at 20 °C overnight.

Seleno-methionine (SeMet)-labeled Tca17 was produced according to the protocol in [34]. Briefly, a preculture of *E. coli* BL21 (DE3)-T1R cells (transformed with GEX6-P1-Tca17) in LB medium was used to inoculate M9 medium supplemented with ampicillin, thiamine and FeSO₄. After reaching an OD₆₀₀ of 0.5, amino-acid synthesis was suppressed by addition of solid amino acids, gene expression was induced by addition of 1 mM IPTG, and cells were grown at 20 °C overnight.

Cell lysate containing Tca17 fused to a glutathione-S-transferase affinity tag at its N-terminus was applied to glutathione Sepharose 4B (GE Healthcare) and, after a wash step with PBS (9.55 g/l Instamed PBS Dulbecco), eluted with 20 mM reduced glutathione (100 mM Tris, pH 8.0). For removal of the GST tag, pooled fractions containing GST-Tca17 were mixed with PreScission™ protease (GE Healthcare) at a ratio of 30:1, and they were dialyzed against 50 mM Tris, 150 mM NaCl and 5 mM 2-mercaptoethanol, pH 8.0 at 4 °C overnight. After loading of the digestion mixture onto a second glutathione Sepharose 4B chromatography column, the flow-through was collected, concentrated and applied to a Superdex® 75 Hiload size exclusion chromatography column that had been equilibrated with 20 mM HEPES, 300 mM NaCl, 2 mM DTT, and 5% v/v glycerol, pH 7.0. For purification of

SeMet-substituted Tca17, the buffer also contained 1 mM EDTA. Fractions containing Tca17 were pooled and concentrated to 12 mg · ml⁻¹ for subsequent experiments.

Crystallization and data collection

Diffraction-quality crystals of full-length Tca17 were grown by the sitting-drop vapor diffusion technique in 100 mM Tris, 200 mM MgCl₂, 15% w/v PEG 3350, pH 8.5 at 4 °C after 2 months. Single crystals were harvested by brief incubation in reservoir buffer including 15% v/v glycerol as cryo-protectant and flash-freezing in liquid nitrogen. Since the Se-Met-labeled crystals of Tca17 diffracted better than the crystals of the native protein, all data sets were collected from the former. Anomalous data (peak, inflection point, high-energy remote) were collected at beamline BL 14.1 of Berliner Elektronensynchrotron (BESSY II, Helmholtz-Zentrum Berlin für Materialien und Energie), while the high-resolution native data set was collected at BL 14.2 of BESSY II. All data were processed using XDS [35]. Data collection statistics are summarized in Table 1.

Structure analysis

MAD data sets were uploaded to and processed with the automatic crystal structure determination pipeline Auto-Rickshaw at EMBL-Hamburg [36]. The resulting electron density map and an initial protein model were used for manual modification and refitting with Coot [37] followed by refinement with Refmac5 [38]. The refined co-ordinates were then used to determine the phases by molecular replacement (MR) of the high-resolution native data set at 1.8 Å. Subsequently, several rounds of manual modification (Coot) and refinement (Refmac5) led to the final model of Tca17 (Table 1). Procheck [39] and MolProbity [40] were used for validation of the deposited model.

Acknowledgements

We thank Marcel Jurk (FMP, Berlin) for analytical ultracentrifugation experiments and staff at BESSY II (Berlin, Germany) for support with the diffraction experiments.

Author information

The atomic co-ordinates as well as the crystallographic structure factors of Tca17 have been deposited in the protein data bank (PDB) under the accession number 3PR6. The authors declare no competing financial interests.

CW planned and performed experiments and analyzed the data; UG analyzed the data and wrote the paper; YR performed experiments; UH planned experiments, analyzed the data and wrote the paper.

References

1. Jahn R, Lang T & Südhof T (2003) Membrane fusion. *Cell* **112**, 519-533.
2. Bonifacino JS & Glick BS (2004) The mechanisms of vesicle budding and fusion. *Cell* **116**, 153-166.
3. Hofmann K-P, Spahn CMT, Heinrich R & Heinemann U (2006) Building functional modules from molecular interactions. *Trends Biochem Sci* **31**, 497-508.
4. Bröcker C, Engelbrecht-Vandré S & Ungermann C (2010) Multisubunit tethering complexes and their role in membrane fusion. *Curr Biol* **20**, R943-R952.
5. Kümmel D & Heinemann U (2008) Diversity in structure and function of tethering complexes: Evidence for different mechanisms in vesicular transport regulation. *Curr Protein Peptide Sci* **9**, 197-209.
6. Whyte JR & Munro S (2002) Vesicle membrane complexes in membrane traffic. *J Cell Sci* **115**, 2627-2637.
7. Yu S & Liang Y (2012) A trapper keeper for TRAPP, its structures and functions. *Cell Mol Life Sci* **69**, 3933-3944.
8. Kümmel D, Oeckinghaus A, Wang C, Krappmann D & Heinemann U (2008) Distinct isocomplexes of the TRAPP trafficking factor coexist inside human cells. *FEBS Letters* **582**, 3729-3733.
9. Jones S, Newman C, Liu F & Segev N (2000) The TRAPP complex is a nucleotide exchanger for Ypt1 and Ypt31/32. *Mol Biol Cell* **11**, 4403-4411.
10. Wang W, Sacher M & Ferro-Novick S (2000) TRAPP stimulates guanine nucleotide exchange on Ypt1p. *J Cell Biol* **151**, 289-296.
11. Cai H, Yu S, Menon S, Cai Y, Lazarova D, Fu C, Reinisch K, Hay JC & Ferro-Novick S (2007) TRAPP I tethers COPII vesicles by binding the coat subunit Sec23. *Nature* **445**, 941-944.
12. Cai H, Zhang Y, Pypaert M, Walker L & Ferro-Novick S (2005) Mutants in trs120 disrupt traffic from the early endosome to the late Golgi. *J Cell Biol* **171**, 823-833.
13. Yamasaki A, Menon S, Yu S, Barrowman J, Meerloo T, Oorschot V, Klumperman J, Satoh A & Ferro-Novick S. (2009) mTrs130 is a component of a mammalian TRAPP II complex, a Rab1 GEF that binds to COPI-coated vesicles. *Mol Biol Cell* **20**, 4205-4215.

14. Kim Y-G, Raunser S, Munger C, Wagner J, Song, Y-L, Cygler M, Walz T, Oh B-H & Sacher M (2006) The architecture of the multisubunit TRAPP I complex suggests a model for vesicle tethering. *Cell* **127**, 817-830.
15. Cai Y, Chin HF, Lazarova D, Menon S, Fu C, Cai H, Sciafani A, Rodgers DW, De La Cruz EM, Ferro-Novick S & Reinisch KM (2008) The structural basis for activation of the Rab Ypt1p by the TRAPP membrane-tethering complexes. *Cell* **133**, 1202-1213.
16. Turnbull AP, Kümmel D, Prinz B, Holz C, Schultchen J, Lang C, Niesen FH, Hofmann K-P, Delbrück H, Behlke J, Müller E-C, Jarosch E, Sommer T & Heinemann U (2005) Structure of palmitoylated human BET3: Insights into TRAPP complex assembly and membrane localization. *EMBO J* **24**, 875-884.
17. Kümmel D, Heinemann U & Veit M (2006) Unique self-palmitoylation activity of the transport protein particle component Bet3: A novel mechanism required for protein stability. *Proc Natl Acad Sci USA* **103**, 12701-12706.
18. Yip CK, Berscheminski J & Walz T (2010) Molecular architecture of the TRAPP II complex and implications for vesicle tethering. *Nature Struct Mol Biol* **17**, 1298-1305.
19. Taussig D, Lipatova Z, Kim JJ, Zhang XQ & Segev N (2013) Trs20 is required for TRAPP II assembly. *Traffic* **14**, 678-690.
20. Lynch-Day MA, Bhandari D, Menon S, Huang J, Cai H, Bartholomew CR, Brumell JH, Ferro-Novick S & Klionsky DJ (2010) Trs85 directs a Ypt1 GEF, TRAPP III, to the phagophore to promote autophagy. *Proc Natl Acad Sci USA* **107**, 7811-7816.
21. Choi C, Davey M, Schluter C, Pandher P, Fang Y, Foster LJ & Conibear E. (2011) Organization and assembly of the TRAPP II complex. *Traffic* **12**, 715-725.
22. Tan D, Cai Y, Wang J, Zhang J, Menon S, Chou H-T, Ferro-Novick S, Reinisch KM & Walz T. (2013) The EM structure of the TRAPP III complex leads to the identification of a requirement for COPII vesicles on the macroautophagy pathway. *Proc Natl Acad Sci USA* **110**, 19432-19437.
23. Montpetit B & Conibear E (2009) Identification of the novel TRAPP associated protein Tca17. *Traffic* **10**, 713-723.
24. Scrivens PJ, Shahrzad N, Moores A, Morin A, Brunet S & Sacher M (2009) TRAPPC2L is a novel, highly conserved TRAPP-interacting protein. *Traffic* **10**, 724-736.
25. Krissinel E & Henrick K (2007) Inference of macromolecular assemblies from crystalline state. *J Mol Bio* **372**, 774-797.

26. Taussig D, Lipatova Z & Segev N (2014) Trs20 is required for TRAPP III complex assembly at the PAS and its function in autophagy. *Traffic* **15**, 327-337.
27. Zong M, Wu X-G, Chan CWL, Choi MY, Chan HC, Tanner JA & Yu S (2011) The adaptor function of TRAPPC2 in mammalian TRAPPs explains TRAPPC2-associated SEDT and TRAPPC9 associated congenital intellectual disability. *PLoS ONE* **6**, e23350.
28. Brunet S, Shahrzad N, Saint-Dic D, Dutczak H & Sacher M (2013) A trs20 mutation that mimics an SEDT-causing mutation blocks selective and non-selective autophagy: A model for TRAPP III organization. *Traffic* **14**, 1091-1104.
29. Sievers F, Wilm A, Dineen DG, Gibson TJ, Karplus K, Li W, Lopez R, McWilliam H, Remmert M, Söding J, Thompson JD & Higgins DG (2011) Fast, scalable generation of high-quality protein multiple sequence alignments using Clustal Omega. *Mol Syst Biol* **7**, 539-545.
30. Ashkenazy H, Erez E, Martz E, Pupko T & Ben-Tal N (2010) ConSurf 2010: Calculating evolutionary conservation in sequence and structure of proteins and nucleic acids. *Nucl Acids Res* **38**, 529-533.
31. Jang SB, Kim YG, Cho YS, Suh PG, Kim KH & Oh BH (2002) Crystal structure of SEDL and its implications for a genetic disease spondyloepiphyseal dysplasia tarda. *J Biol Chem* **277**, 49863-49869.
32. Gedeon AK, Tiller GE, LeMerrer M, Heuertz S, Tranebjaerg L, Chitayat D, Robertson S, Glass IA, Savarirayan R, Cole WG, Rimoin DL, Kousseff BG, Ohashi H, Zabel B, Munnich A, Géczy J & Mulley JC (2001) The molecular basis of X-linked spondyloepiphyseal dysplasia tarda. *Am J Hum Genet* **68**, 1386-1397.
33. Shaw A, Brunetti-Pierrri N, Kádasi L, Kováčová V, Van Maldergem L, De Brasi D, Salerno M & Géczy J (2003) Identification of three novel SEDL mutations, including mutation in the rare, non-canonical splice site of exon 4. *Clin Genet* **64**, 235-242.
34. Van Duyne GD, Standaert RF, Karplus PA, Schreiber SL & Clardy J (1993) Atomic structures of the human immunophilin FKBP-12 complexes with FK506 and rapamycin. *J Mol Bio.* **229**, 105–124.
35. Kabsch W (2010) XDS. *Acta Crystallogr D* **66**, 125-132.
36. Panjikar S, Parthasarathy V, Lamzin VS, Weiss MS & Tucker PA (2005) Auto-rickshaw: An automated crystal structure determination platform as an efficient tool for the validation of an X-ray diffraction experiment. *Acta Crystallogr D* **61**, 449-457.
37. Emsley P, Lohkamp B, Scott WG & Cowtan K (2010) Features and development of Coot. *Acta Crystallogr D* **66**, 486-501.

38. Murshudov GN, Skubak P, Lebedev AA, Pannu NS, Steiner RA, Nicholls RA, Winn MD, Long F & Vagin AA (2011) REFMAC5 for the refinement of macromolecular structures. *Acta Crystallogr D* **67**, 355-367.
39. Laskowski RA, MacArthur MW, Moss DS & Thornton JM (1993) PROCHECK: A program to check the stereochemical quality of protein structures. *J Appl Cryst* **26**, 283-291.
40. Chen VB, Arendall WB, Headd JJ, Keedy DA, Immormino RM, Kapral GJ, Murray LW, Richardson JS & Richardson DC (2010) MolProbity: All-atom structure validation for macromolecular crystallography. *Acta Crystallogr D* **66**, 12-21.
41. Collaborative Computational Project, Number 4 (1994) The CCP4 suite: Programs for protein crystallography. *Acta Crystallogr D* **50**, 760-763.
42. Baker NA, Sept D, Joseph S, Holst MJ & McCammon JA (2001) Electrostatics of nanosystems: application to microtubules and the ribosome *Proc Natl Acad Sci USA* **98**, 10037-10041.
43. The PyMOL Molecular Graphics System, Version 1.7 Schrödinger, LLC.

Tables

Table 1. Crystallographic data collection and model refinement statistics

^aData for the highest resolution shell in parenthesis, ^bCalculated with BAVEGAGE [41], ^cCalculated with MOLPROBITY [40], ^dClashscore is the number of serious steric overlaps (> 0.4 Å) per 1000 atoms.

Data Collection				
Data sets	Peak	Inflection point	Remote	Native
Wavelength [Å]	0.9797	0.9798	0.9720	0.9184
Temperature [K]	100			
Space group	C2			
Unit cell parameters				
a, b, c [Å]	57.24, 46.75, 50.48			57.13, 58.49, 53.97
β [°]	92.92			92.62
Resolution range [Å] ^a	28.96-3.12 (3.20-3.12)	29.93-2.99 (3.07-2.99)	29.09-3.11 (3.19-3.11)	29.25-1.80 (1.85-1.80)
Reflections ^a				
Unique	4558 (323)	5235 (396)	4659 (342)	16453 (1216)
Completeness [%]	98.1 (99.1)	98.1 (95.4)	97.9 (100.0)	99.4 (99.5)
Multiplicity	1.7	1.7	1.7	3.2
Data quality ^a				
Intensity <I/σ(I)>	11.3 (2.3)	11.8 (1.6)	11.4 (1.9)	17.5 (3.0)
R _{meas} [%]	6.4 (48.4)	5.8 (65.2)	6.4 (51.0)	4.7 (47.4)
Wilson B value [Å ²]	58.9	65.6	66.5	35.31
Refinement				
Resolution range [Å] ^a	29.25-1.80 (1.85-1.80)			
Reflections ^a				
Number	15631 (1127)			
Completeness [%]	99.3 (97.8)			
Test set (5%)	823(59)			
R _{work}	18.32 (20.30)			

R _{free}	21.96 (24.70)
Contents of the asymmetric unit	
Protein: Molecules, residues, atoms	1, 143, 1164
Ligands: Molecules, atoms	2, 7
Water: Molecules	133
Mean displacement factors [Å ²] ^b	
All atoms	31.76
Protein	31.89
Ligands	65.66
Water oxygens	28.80
RMSD from target geometry	
Bond lengths [Å]	0.011
Bond angles [°]	1.277
RMSD displacement factors [Å ²] ^b	
Main chain	0.731
Side chain	2.186
Estimated mean coordinate error [Å]	
Based on R _{free}	0.025
Based on maximum likelihood	0.069
Validation statistics ^c	
Ramachandran map	
Residues in favored regions [%, No.]	100.0, 143
MOLPROBITY Clashscore ^d	4.1

Figure Legends

Fig. 1. Cartoon representation of full-length Tca17, colored in a rainbow scheme from the N-terminus (dark blue) to the C-terminus (red). **(A)** As seen from the one-helix side, **(B)** after rotation of 180°, the molecule is shown from the two-helix side. Secondary structure elements (α -helices and β -strands) are labeled. Dashed sections of the chain could not be modeled due to local disorder.

Fig. 2. ConSurf color-coded multiple sequence alignment [30] of Tca17/TRAPPC2L orthologs. Amino acid sequences are shown in the one-letter code. The degree of conservation is shown from variable (1, dark cyan) to conserved (9, dark magenta). Yellow letters indicate an insufficient number of residues that can be aligned (less than 10%). Regions that form continuous patches on the surface of Tca17 (see Fig. 3B) are marked as red boxes.

The following Tca17 orthologs were included in the alignment (**UniProt ID**): **Q753D1_ASHGO**: Hypothetical protein from *Ashbya gossypii*, **Q6CJQ8_KLULA**: Hypothetical protein from *Kluyveromyces lactis*, **C5DXJ3_ZYGRC**: Hypothetical protein from *Zygosaccharomyces rouxii*, **TPC2L_BOVIN**: TRAPPC2L from *Bos taurus*, **C4XWA9_CLAL4**: Hypothetical protein from *Clavispora lusitaniae*, **TPC2L_SALSA**: TRAPPC2L from *Salmo salar*, **Q6FLS1_CANGA**: Tca17-like protein from *Candida glabrata*, **C4R7P1_PICPG**: Hypothetical protein from *Pichia pastoris*, **TPC2L_DICDI**: TRAPPC2L from *Dictyostelium discoideum*, **TPC2L_HUMAN**: TRAPPC2L from *Homo sapiens*, **TPC2L_MOUSE**: TRAPPC2L from *Mus musculus*, **A7TN14_VANPO**: Hypothetical protein from *Vanderwaltozyma polyspora*, **TPC2L_RAT**: TRAPPC2L from *Rattus norvegicus*, **TPC2L_TAEGU**: TRAPPC2L from *Taeniopygia guttata*, **TCA17_YEAST**: Tca17 from *Saccharomyces cerevisiae*, **C5DDR2_LACTC**: Hypothetical protein from *Lachancea thermotolerans*, **TPC2L_PONAB**: TRAPPC2L from *Pongo abelii*, **TPC2L_XENTR**: TRAPPC2L from *Xenopus tropicalis*.

Fig. 3. Sequence conservation of Tca17. Eighteen Tca17/TRAPPC2L ortholog proteins were aligned, and the sequence conservation was calculated by ConSurf [30]. **(A)** Ribbon representation of Tca17 seen from the one-helix (left) and the two-helix (right) side. The coloring scheme corresponds to ConSurf scores ranging from variable (dark cyan) to conserved (dark magenta). Regions that are insufficiently represented within the set of orthologs are colored yellow. **(B)** Surface representation of Tca17. Orientations and coloring scheme as in (A). Two distinct, highly conserved patches are marked by dashed lines.

Fig. 4. Electrostatic surface potential across the Bet5 protein family. Shown are Tca17 (**PDB ID: 3PR6**, this study), Bet5 (**PDB ID: 3CUE**, chain C), Sedlin (**PDB ID: 2J3W**, chain A) and Trs23 (**PDB ID: 3CUE**, chain A). All proteins are shown from the one-helix side (upper panel) and the two-helix side (lower

panel). The potential was calculated using APBS [42] and mapped onto the solvent-accessible surface by Pymol [43] between +3.0 kT/e (blue) and -3.0 kT/e (red).

Fig. 5. Conserved patch 1 (see Figs. 2, 3) in Sedlin and Tca17. Superposition of Sedlin (cyan) and Tca17 (magenta) shown from the one-helix side. The two conserved residues L44 and D45 of Tca17 (L46/D47 in Sedlin) are shown as sticks. (Insert) Detail of patch 1.

Fig. 6. Putative Integration of Tca17 into TRAPP. **(A)** Composite model for the TRAPP I complex from yeast. The complex was modeled by combining structural information from the mammalian Bet3-Trs31-Sedlin complex [14], the mammalian Bet3-Tpc6A-Bet5-Trs23 complex [14], and the minimal sub-complex of yeast TRAPP I required for Ypt1 GEF activity [15]. Yeast TRAPP I model as seen from the putative membrane facing side. Two possible positions are shown for Tca17 (red), with Tca17-A replacing Sedlin (Trs20 in yeast) and Tca17-B being an additional subunit. In the mammalian complex structures, Sedlin (white ribbon representation) binds to Bet3 (yellow) and Trs31 (orange). The suggested positions of Tca17 in the yeast complex were found through superposition by secondary-structure-matching in Coot [37].

(B) Replacement of Sedlin (Trs20 in yeast) by Tca17 changes the electrostatic surface potential of TRAPP. The TRAPP I model shown in (A) was used for calculation of the potential with APBS and Pymol (see Fig. 4) between +3.0 kT/e (blue) and -3.0 kT/e (red). TRAPP I model containing Sedlin (dashed box), membrane-facing side. **(C)** TRAPP I model with Tca17 (dashed boxes) added to the complex (Tca17-B) or docked into the position occupied by Sedlin (Tca17-A). Shown are the membrane-facing side (top) as well as a side view (bottom).

Fig. 7. The Bet3-interacting motifs of Sedlin and Tca17. **(A)** The interface of Sedlin and Bet3 [14]. Surface representation of Bet3 (orange) with residues within 4.5 Å distance from Sedlin in blue. Sedlin is shown in yellow with residues involved in Bet3 interaction as stick models. **(B)** The Bet3 interaction motif of Sedlin. **(C)** Putative Bet3-interaction motif of Tca17.

Fig. 8. Electrostatic surface potential across the putative interfaces of Tca17-binding subunits of TRAPP. Shown are Trs33 (PDB ID: 2J3T, chain B), Tca17 (PDB ID: 3PR6, this study,), and Trs31 (PDB ID: 2J3W, chain B). Sedlin (PDB ID: 2J3W) is shown for comparison. The potential was calculated using APBS and Pymol (see Fig. 4) between +3.0 kT/e (blue) and -3.0 kT/e (red). Individual interfaces are outlined in black.

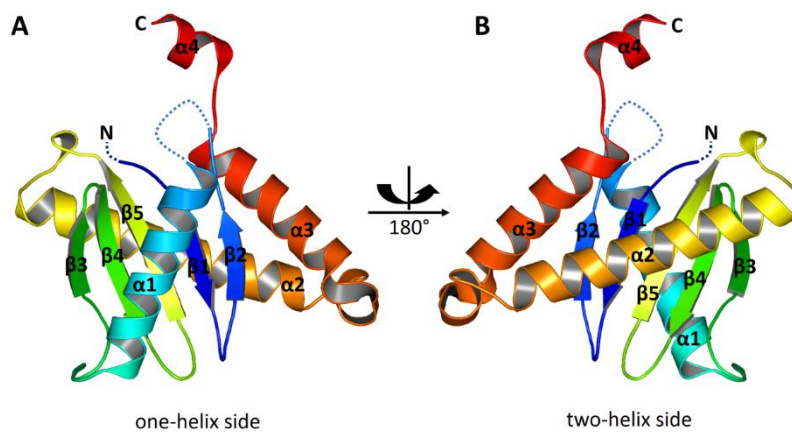


Figure 1

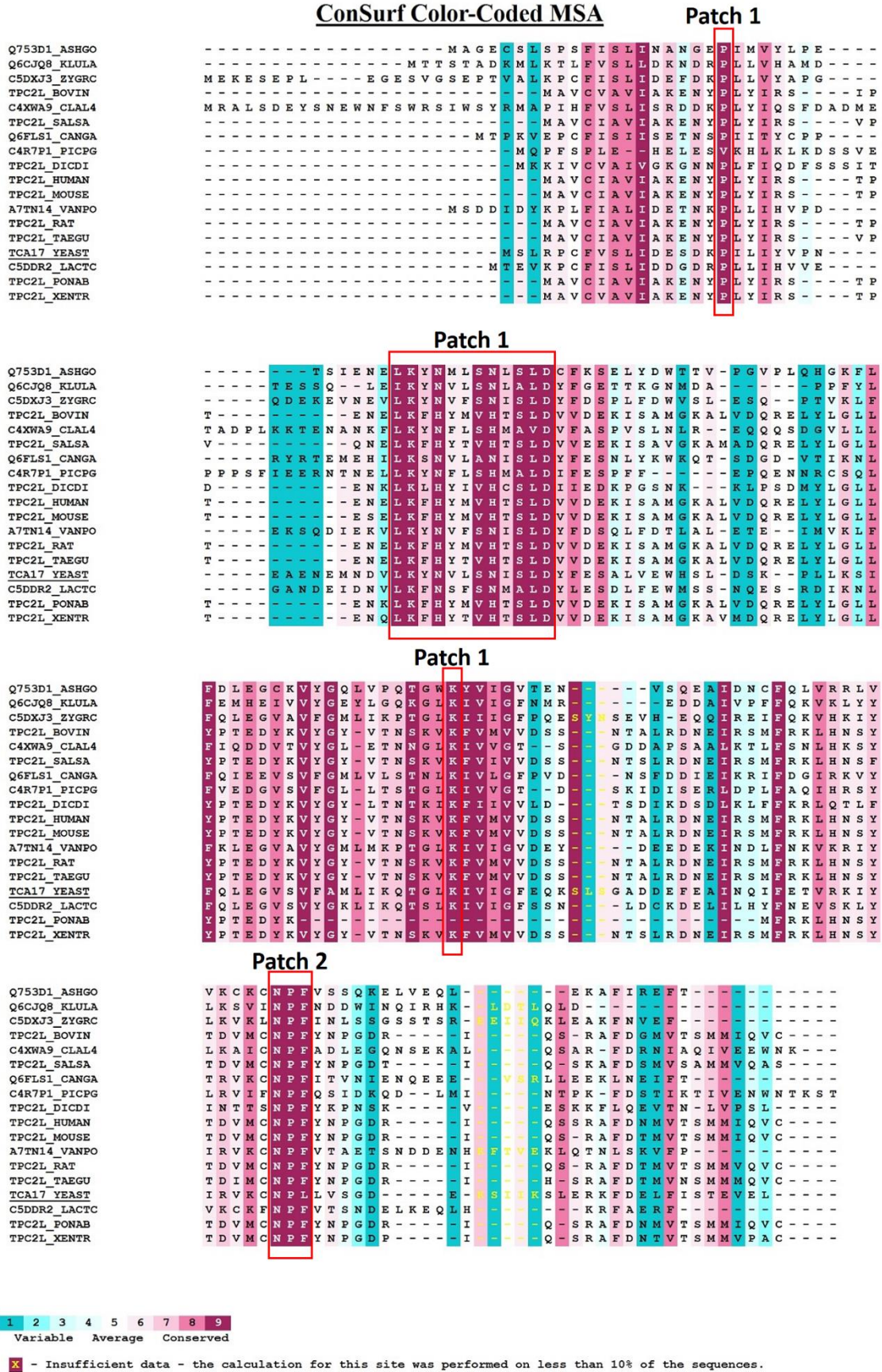


Figure 2

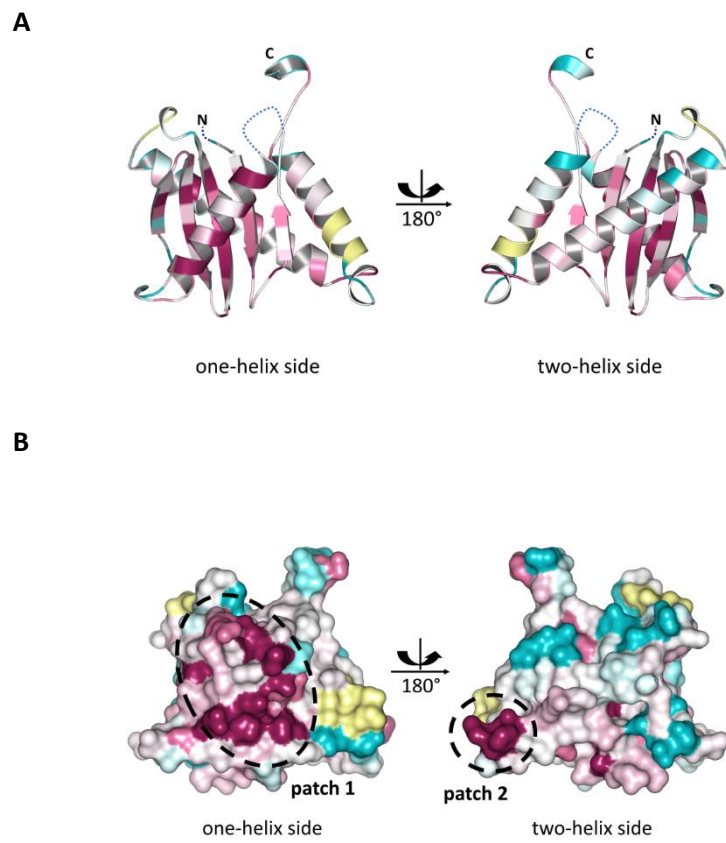


Figure 3

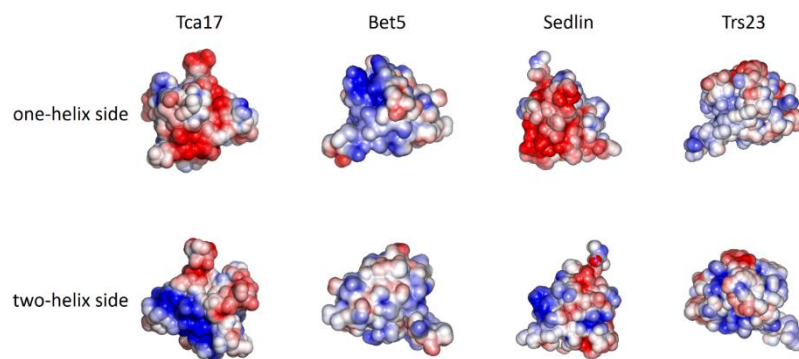


Figure 4

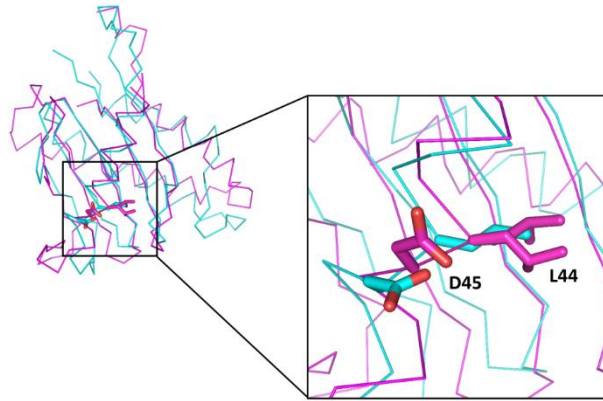


Figure 5

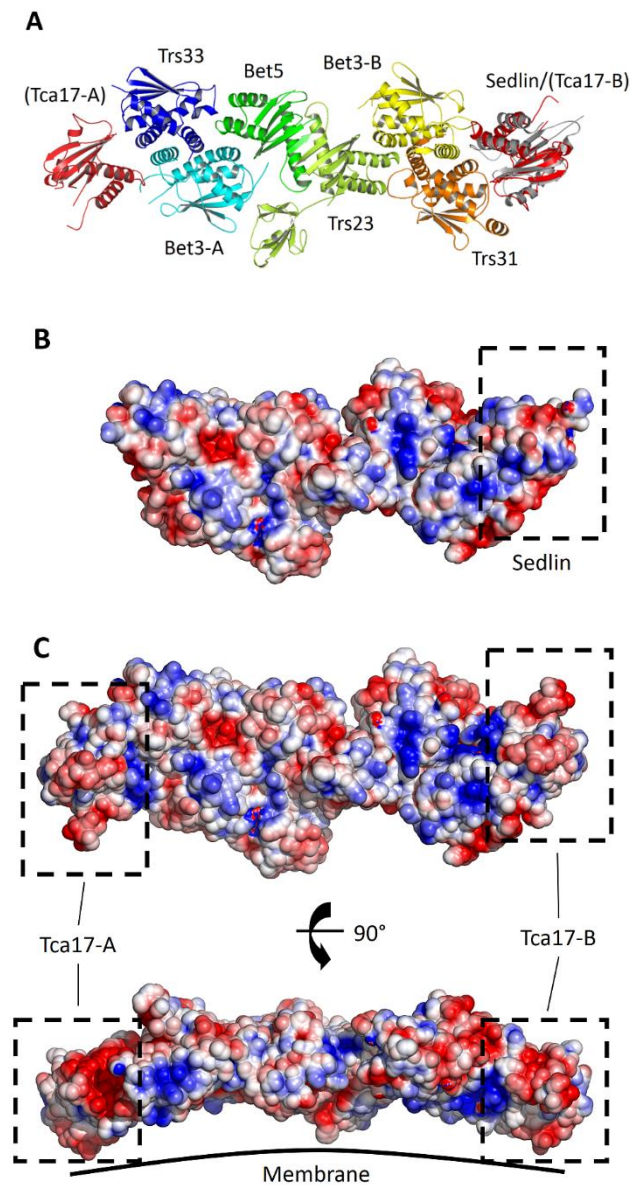


Figure 6

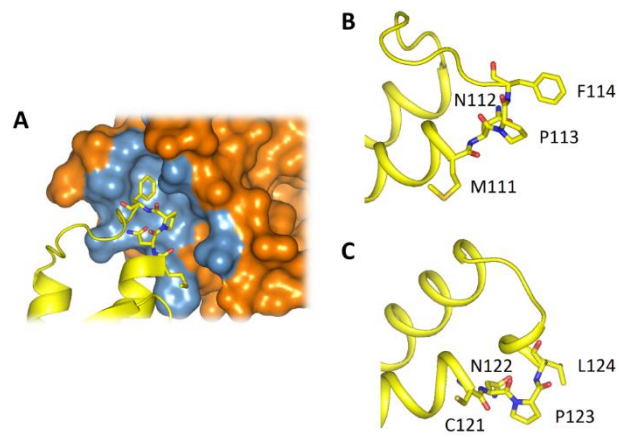


Figure 7

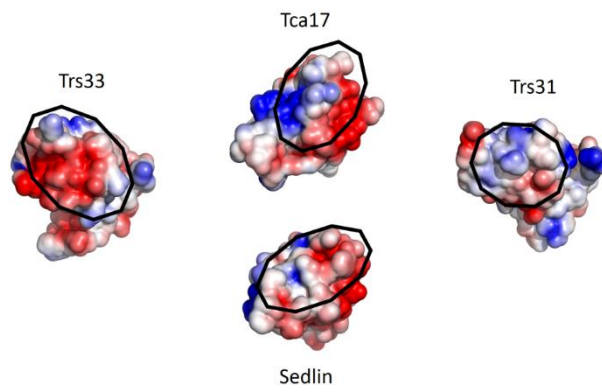


Figure 8